Joint Assignment and Scheduling for Minimizing Age of Correlated Information

Qing He, *Member, IEEE,* György Dán, *Senior Member, IEEE,* and Viktoria Fodor, *Senior Member, IEEE*

***Abstract*—Age of information has been recently proposed to quantify the freshness of information, e.g., in cyber-physical systems, where it is of critical importance. Motivated by wireless camera networks where multi-view image processing is required, in this paper we propose to extend the concept of age of information to capture packets carrying correlated data. We consider a system consisting of wireless camera nodes with overlapping fields of view and a set of processing nodes, and address the problem of the joint optimization of processing node assignment and camera transmission scheduling, so as to minimize the maximum peak age of information from all sources. We formulate the multi-view age minimization (MVAM) problem, and prove its NP-hardness under the two widely used interference models as well as with given candidate transmitting groups. We provide fundamental results including tractable cases and optimality conditions of the MVAM problem for two baseline scenarios. To solve MVAM efficiently, we develop an optimization algorithm based on a decomposition approach. Numerical results show that by employing our approach the maximum peak age is significantly reduced in comparison to a traditional centralized solution with minimum-time scheduling.**

***Index Terms* – Age of information, correlated information, optimization, wireless camera networks.**

I. Introduction

Wireless camera networks acquire, process, and analyze digital images of areas or objects of interest. They form an important building block of future smart cities, and serve a variety of applications, such as surveillance [1], tracking [2], healthcare [3], and intelligent transportation [4]. Many of these applications require multiple cameras with overlapping fields of view (FoV) to monitor a given scene, as doing so can improve the robustness and accuracy of tracking, and enables 3D scene reconstruction. Images from cameras with overlapping FoVs have to be processed jointly, and under strict delay constraints to enable real-time operation. The emerging paradigm of fog computing could enable meeting the strict delay constraints, as it allows to distribute computation, communication, control and storage to computing nodes close to the cameras, referred to as fog nodes. Comparing to centralized cloud-based systems, fog computing based solutions reduce the network traffic and delay, while they remain compatible with affordable low cost cameras. Still, real-time processing of the visual information in a fog computing enabled wireless camera system requires joint optimization of the allocation of computing resources and the scheduling of images from cameras transmitting over a shared wireless channel.

Q. He, G. Dán, and V. Fodor are with the Division of Network and Systems Engineering, School of Electrical Engineering and Computer Science, KTH Royal Institute of Technology, SE-10044, Stockholm, Sweden. (e-mail: {qhe,gyuri,vfodor}@kth.se).

The work was partly funded by the Swedish Research Council through project 621-2014-6.

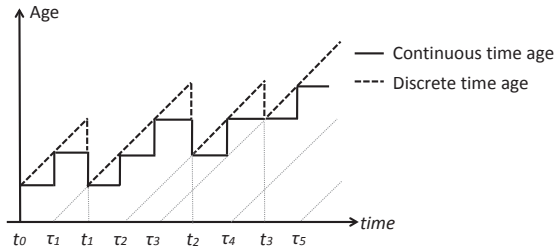

Fig. 1. Age evolution of a source. The i^{th} packet with time stamp τ_i is received by the destination at t_i. The age at t_i equals $t_i - \tau_i$. If no packet is received, the age increases linearly.

A promising metric for quantifying the timeliness of end-to-end data delivery, including queuing and transmission times, is the recently introduced age of information, or simply, age [5]. Age is commonly defined as the time elapsed since the most recently received message was generated (see [6] and references therein), as shown in Figure 1.

By definition, the value of age changes upon receiving each packet. However, when processing requires information from multiple senders, carried in different packets, such as the case of cameras with overlapping FoVs, age of information should change only when all packets carrying correlated information are received. Extending the notion age to the context of wireless camera networks thus requires us to revisit the way of defining and calculating age: age has to be defined as the difference between the current observation time and the generation time of the latest "fully" received correlated set of packets. In Figure 2, we illustrate age evolution of a source given this new definition. We remark that the packets carrying correlated information may be not delivered consecutively since they are sent from multiple transmitters.

In order to minimize the age of information in a wireless camera network, we need to solve two coupled resource allocation problems. First, we need to determine the serving fog node for each camera. We refer to this as the *camera-node assignment*. Second, we need to to decide which of the mutually interfering cameras should transmit together and for how long. We refer to this as *camera transmission scheduling*. Clearly, the two problems are coupled and require joint optimization in order to minimize the age of the multi-view image data at the fog nodes.

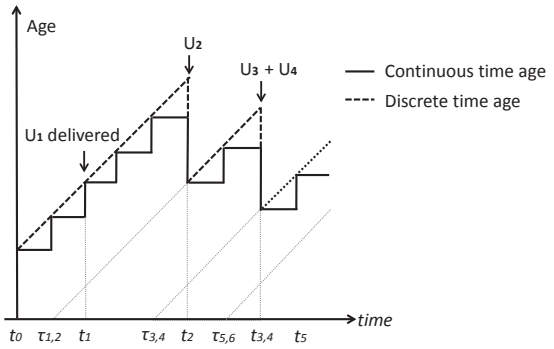

Fig. 2. Age evolution of correlated information of a source. Packets U_1 and U_2 carrying correlated information were generated at $\tau_{1,2}$ and received by the destination node at t_1 and t_2, respectively. The age increases linearly until t_2, when it decreases to $t_2 - \tau_{1,2}$. After t_2, the age increases linearly until $t_{3,4}$, when packets U_3 and U_4 carrying correlated information and with time stamp $\tau_{3,4}$ were simultaneously received by the destination. The age at $t_{3,4}$ equals $t_{3,4} - \tau_{3,4}$.

A. Related Work

The study on age of information has received large attention since the concept was formally introduced [5]. Early works show that age is different from existing metrics, such as delay and latency. Hence it is a fundamentally novel metric quantifying the freshness of information (see [6] and the references therein). In most of previous works, e.g., [5]–[8], the problem of age in different real-time systems has been explored using various queueing models like M/M/1, M/M/2, M/D/1, M/G/1, etc., where status update packets arrive stochastically at the source nodes and are queued following the discipline of First-Come-First-Served (FCFS). New queue management strategies, e.g., Last-Come-First-Served (LCFS), were proposed in [9], [10]. The authors of [11] show that the LGFS policy achieves a smaller age process (in a stochastic ordering sense) than any other causal policy for multi-channel and multi-hop networks. In [12], a general age penalty function was introduced to characterize the level of dissatisfaction on data staleness. To evaluate the timeliness for a system in question, the average age, calculated as the area under the sawtooth curve in Figure 1, normalized by the observation interval, was considered in [5], [7] for capturing the average system behavior in a queueing system fed by a single source and by multiple sources, respectively. To characterize the worst case system behavior, the authors of [10] introduced the notion of peak age, which is the maximum value of the age achieved immediately before receiving a new packet (e.g., in Figure 1, the i^{th} peak age of the source is obtained observing the i^{th} peak value in the sawtooth curve). Subsequently, [13] considered optimal link scheduling to drain a given set of packets with respect to the total age. In [14], a stationary scheduling policy has been proposed for minimizing average and peak age in wireless networks under general interference constraints. In all these works, the age of information changes upon receiving each individual packet. Therefore, existing results do not apply for camera networks with multi-view processing, as considered in our work.

Wireless camera networks (or visual sensor networks) have been studied extensively in the past two decades, with the main objective of improving the quality of visual analysis and to enable real-time service, subject to the inherent communication and computing resource constraints. Recently, wireless camera networks have been revisited in the context of fog computing architectures [15]. In [16], the authors address the multi-view sensor assignment problem with the objective of maximizing the total number of multi-views processed within a time frame, and present an approximation algorithm. In [17] the minimization of the time needed to complete the distributed visual analysis for a video sequence subject to a mean average precision requirement is considered. The problem of multi-view coding and routing of features in visual sensor networks is studied in [18], where the authors develop a robust optimization framework for maximizing the amount of information extracted from the sources. Nevertheless, the communication and computing resource allocation in wireless camera (or visual sensor) networks with respect to the freshness of information has not been considered until recently [19]. Compared to [19], where we address the joint optimization problem for the uncapacitated fog node case and present basic results, in this paper we consider the capacitated fog node case, and significantly extend both the analytical and the numerical results.

B. Contributions

In this paper, we propose to jointly optimize fog node assignment and transmission scheduling in a wireless camera network, so as to minimize the age of the multi-view image data at the destinations. Our main contributions are fourfold. First, we extend the concept of age of information to correlated information from multiple senders, which allows us to use this metric in wireless camera networks. Beyond wireless camera networks, our proposed notion of age can be used in other systems where an age update is triggered by multiple correlated packets. Second, we consider the joint optimization of fog node assignment and camera transmission scheduling, so as to minimize the age of the multi-view image data at the fog nodes. We formulate the optimization problem and provide fundamental results about problem complexity, tractable cases, and optimality conditions. Third, to efficiently solve the problem, we develop a sub-optimal, but fast, algorithm based on problem decomposition. In addition, for benchmarking purposes, we provide an integer linear programming (ILP) formulation, which enables the computation of global optima for small problem instances. Finally, we use simulations to explore the benefits of the jointly optimized fog node assignment and camera transmission strategy for minimizing the age of information in wireless camera networks.

II. System Model and Problem Formulation

A. Camera network with multi-view processing

We consider a wireless camera network that consists of a set of cameras $\mathcal{C} = \{1, 2, \ldots, C\}$, a set of scenes $\mathcal{S} = \{1, 2, \ldots, S\}$, which we also refer to as sources, and a set of fog (computing) nodes $\mathcal{N} = \{1, 2, \ldots, N\}$. Each camera captures images from one of the scenes. The cameras have overlapping FoV, and each scene is monitored by multiple

cameras. We denote by $\mathcal{c}(s)$ the set of cameras that have a view of scene s, and we assume that cameras monitoring the same scene capture images simultaneously. The cameras send the images to their respective serving fog node for processing, and we define

$$l_{cn} = \begin{cases} 1 & \text{if camera } c \text{ is served by node } n; \\ 0 & \text{otherwise.} \end{cases} \quad (1)$$

To allow the processing of multi-views, the cameras $\mathcal{c}(s)$ that cover scene s need to transmit their images to the same fog node, hence we have

$$\sum_{n\in N} \prod_{c\in\mathcal{c}(s)} l_{cn} = 1, \ \forall s \in \mathcal{S}. \quad (2)$$

The fog nodes are responsible for receiving and processing the image data from the cameras they serve. The information from one scene is processed by one fog node. To capture computing capacity constraints, we denote by M_n the maximum number of cameras that can be supported by fog node n, that is,

$$\sum_{c\in\mathcal{C}} l_{cn} \le M_n, \ \forall n \in \mathcal{N}. \quad (3)$$

The images captured by a camera are queued in its buffer before being delivered to the respective fog node. We consider the first-come-first-served (FCFS) queueing discipline, because in applications such as monitoring and tracking historical data are of interest as well and hence need to be delivered in a timely manner.

The cameras transmit the images to the fog nodes via a shared wireless channel, as depicted in Figure 3. To determine whether or not a set of cameras can transmit simultaneously, we consider two widely used interference models [20]. Under the protocol model any two camera-fog node pairs can be active together if and only if they are sufficiently spatially separated from each other. Under the physical model, aka, the signal-to-interference-and-noise ratio (SINR) model, for a subset of cameras $\mathcal{g} \subseteq \mathcal{C}$ to be able to transmit together, given SINR thresholds must be met at each fog node serving the cameras,

$$\text{SINR}_n(c,\mathcal{g}) \triangleq \frac{P_c G_{cn}}{\sum_{\iota\in\mathcal{g},\iota\neq c} P_\iota G_{\iota n} + \sigma_n^2} \ge \gamma_c, \quad (4)$$
$$n \in \{\mathcal{N} : l_{cn} = 1\}, \ \forall c \in \mathcal{g},$$

where P_c is the transmit power of camera c and G_{cn} is the channel gain between camera c and fog node n, incorporating the effects of path loss, shadowing and fading, and σ_n^2 is the noise variance. In what follows, to achieve a unified problem formulation, we use the term *group* to refer to a set of cameras that can transmit simultaneously, determined by the interference model. We denote by $\mathcal{g}$ a camera group and by Ψ the set of all feasible camera groups under a given interference model and network configuration, then $\mathcal{g} \in \Psi$.

B. Age calculation

We consider that time is slotted and is divided into subsequent scheduling cycles. In each scheduling cycle, we schedule the transmission of the images queued at the beginning of the cycle. We denote by U_{ci} the i^{th} image in the queue of camera c. The images that arrive during the cycle are queued by the cameras under the FCFS discipline, and will be scheduled in the next cycle. The considered cycle-based scheduling is motivated by scenarios where the information updates happen at random, e.g., triggered by environmental changes, and thus the arrival of new packet is hard to predict. Nonetheless, it also a useful model for scenarios where arrivals are predictable, in which case the cycle length and the re-scheduling frequency could be optimized (often referred to as a receding horizon control strategy).

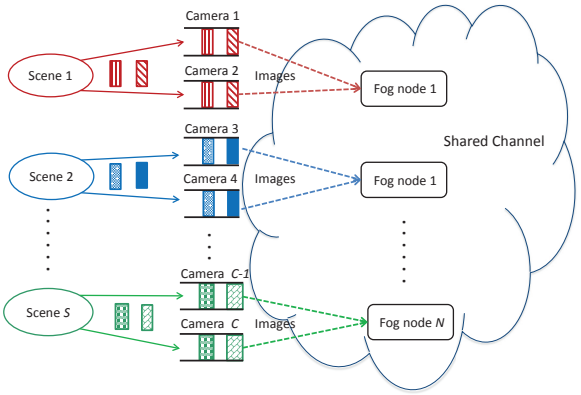

Fig. 3. An illustration of the system model, where each scene is monitored by at least two cameras, as indicated by the solid lines, and each camera transmits the captured images to its destination fog node, as shown by the dashed lines.

Let us denote by t_0 the starting time of the current scheduling cycle, and by K_c the number of queued images of camera c at t_0. Furthermore, we denote by t_j the time at the end of the j^{th} slot of the scheduling cycle. The transmission rate of a camera-fog node pair in a feasible group is one image per time slot. Since the image data are queued using FCFS and the cameras monitoring the same scene capture images simultaneously, the i^{th} image in the queue of each camera $c \in \mathcal{c}(s)$ carries time stamp τ_{si}, which indicates the generation time of image U_{ci}, $\forall c \in \mathcal{c}(s)$. We refer to the set of images $B_{si} = \{U_{ci}, \forall c \in \mathcal{c}(s)\}$ as the i^{th} image block of s.

Let us denote by a_{s0} the initial age of scene s at time t_0. Due to the requirement of multi-view processing, the information of scene s will not be updated until all the images of an image block are delivered to the fog node n serving cameras $\mathcal{c}(s)$. Therefore, at time t_j the age of a source s is defined as

$$a_{sj} = \begin{cases} t_j - \tau_{si} & \text{if all the images of the } i^{th} \text{ image} \\ & \text{block of } s \text{ have been delivered to} \\ & \text{node } n \text{ exactly by } t_j; \\ a_{s,j-1} + 1 & \text{otherwise.} \end{cases} \quad (5)$$

Note that the age calculation in (5) differs from the case when the age is updated upon the delivery of each packet, as considered in the literature. In addition, it may happen that the images in an image block are not delivered consecutively since they are sent from multiple cameras. Hence our problem differs from the case when multiple (consecutive) time slots are occupied to deliver one image. An example will be provided later in Section II-C.

To deliver the queued images as timely as possible as well as for fairness among the sources, we are interested in minimizing the maximum peak age of all scenes. By the definition in (5), the peak ages of a scene are attained immediately before the last image of an image block is delivered to its serving fog node. To express the peak ages, let us denote by t_{ci} the time when image U_{ci} is delivered, and by $T_{ci} = t_{ci} - t_0$ the number of time slots before U_{ci} is delivered, and observe that T_{ci} is a positive integer in $[1, \sum_{c\in\mathcal{C}} K_c]$. Then by defining $\tau_{s0} = t_0 - a_{s0}$, we can express the i^{th} peak age of s as $\alpha_s^i = \max_{c\in\mathcal{c}(s)} t_{ci} - \tau_{s,i-1} = t_0 + \max_{c\in\mathcal{c}(s)} T_{ci} - \tau_{s,i-1}$.

C. Problem Formulation

In order to optimize the worst case performance, we formulate the multi-view age minimization (MVAM) problem as that of minimizing the maximum peak age of all sources in a scheduling cycle,

$$\underset{\{T_{ci}\in Z^+,\ l_{cn}\in\{0,1\}\}}{\text{minimize}} \quad \max_{s\in\mathcal{S},\ c\in\mathcal{c}(s),\ i=1,\ldots,K_c} \alpha_s^i \tag{6a}$$

subject to (2), (3), and

$$\alpha_s^i = t_0 + \max_{c\in\mathcal{c}(s)} T_{ci} - \tau_{s,i-1} \quad \forall s\in\mathcal{S},\ i=1,\ldots,K_c, \tag{6b}$$

$$1 \le T_{c1} < T_{c2} < \cdots < T_{c,K_c} \quad \forall c\in\mathcal{C}, \tag{6c}$$

$$\mathcal{g}_j \in \Psi \quad \mathcal{g}_j = \{c\in\mathcal{C} : T_{ci} = T_j, i=1,\ldots,K_c\}, \quad T_j = 1,\ldots,\sum_{c\in\mathcal{C}} K_c. \tag{6d}$$

Observe that solving MVAM requires joint optimization of the camera to fog node assignment, and of the transmission schedule of the cameras to their serving fog nodes. We remark that at the optimum of (6), if the scheduling solution uses T time slots and $T < \sum_{c\in\mathcal{C}} K_c$, then $\mathcal{g}_j$ are empty sets for $j = \{T+1,\ldots,\sum_{c\in\mathcal{C}} K_c\}$. Hence in (6d), T can be overestimated without loss of optimality. The candidate group set Ψ is determined by the interference model as well as the camera-node assignment. For the MVAM under the physical model, following the SINR constraint in (4), the constraint set (6d) can be written as

$$\begin{aligned} &\text{SINR}_n(c,\mathcal{g}_j) = \frac{P_c G_{cn}}{\sum_{\iota\in\mathcal{g}_j,\iota\neq c} P_\iota G_{\iota n} + \sigma_n^2} \ge \gamma_c,\ \forall c\in\mathcal{g}_j, \\ &n\in\{\mathcal{N} : l_{cn}=1\},\ T_j = 1,\ldots,\sum_{c\in\mathcal{C}} K_c, \\ &\mathcal{g}_j = \{c\in\mathcal{C} : T_{ci} = T_j, i=1,\ldots,K_c\}. \end{aligned} \tag{7}$$

We summarize the key notation in Table I.

D. Integer Linear Programming Formulation

The formulation of MVAM in (6) is non-linear and non-convex. By applying non-trivial linearization techniques we develop an integer linear programming (ILP) formulation of the MVAM and present it in Appendix A. The ILP could be used for performance benchmarking as it enables efficient computation of global optima for problem instances of small and moderate sizes using off-the-shelf solvers [21], [22].

We end this section by providing an MVAM instance, for which in the optimal solution the images from a block are not delivered consecutively, as illustrated in Figure 4. The example shows that the MVAM is more complex than the case where the information updates are independent, and further motivates the theoretical investigation of complexity and the structural results that follow.

TABLE I

Notation	Description
$\mathcal{S}$	the set of scenes
$\mathcal{C}$	the set of cameras
$\mathcal{N}$	the set of fog nodes
$\mathcal{c}(s)$	The subset of cameras monitoring scene s
$\mathcal{g}$	A subset of cameras that can transmit together
Ψ	The union of all compatible camera sets, or groups
M_n	The maximum number of cameras served by node n
t_0	The initial time
t_j	The time corresponds to the end of the j^{th} time slot
K_c	The number of queued images in camera c
U_{ci}	The i^{th} image of camera c
τ_{si}	The time stamp carried by U_{ci}, $\forall c\in\mathcal{c}(s)$
B_{si}	the i^{th} image block of s
a_{s0}	The initial age of s at t_0
a_{sj}	The age of s at t_j
α_s^i	The i^{th} peak age of s
T_{ci}	The number of slots before U_{ci} is delivered

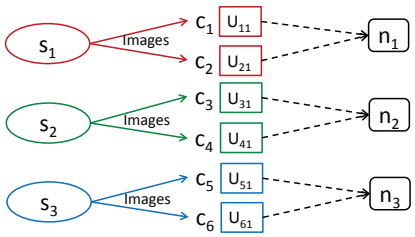

Fig. 4. A camera network with scenes $\mathcal{S} = \{s_1, s_2, s_3\}$, each covered by two cameras as indicated by the solid lines, and fog nodes $\mathcal{N} = \{n_1, n_2, n_3\}$, each supporting at most two cameras. The initial ages satisfy $a_{10} > a_{20} > a_{30}$. Each camera has one image to be delivered. The interference model is such that the only feasible (and hence optimal) camera-node assignment is as shown by the dashed lines, and the cameras groups are $\{c_1, c_2, c_5\}$, $\{c_3, c_4\}$, and $\{c_6\}$. One can verify that at the optimum, the transmission schedule is to transmit the camera groups $\{c_1, c_2, c_5\}$, $\{c_3, c_4\}$, and $\{c_6\}$ in sequence, each occupying one slot. In the optimal solution, correlated images U_{51} and U_{61} are not delivered consecutively.

III. MVAM Complexity

The MVAM is a combinatorial optimization problem. In the following theorems, we prove the NP-hardness of the MVAM problem under the two interference models as well as with given candidate group sets.

Theorem 1. *The MVAM under the physical model is NP-hard.*

Proof: The decision problem of the MVAM is to determine whether or not there exists a solution such that the maximum peak age is no more than a given value. We show that the decision problem is NP-complete by constructing a polynomial-time reduction from the 3-satisfiability (3-SAT) problem, which is one of Karp's 21 NP-complete problems [23].

For an irreducible instance of the 3-SAT problem, let us denote by $\mathcal{S}$ and $\mathcal{S}'$ the set of its positive literals and its negative literals, respectively. The set of clauses is denoted

by $\mathcal{D}$. We construct an MVAM instance with $|\mathcal{S}|+|\mathcal{D}|$ scenes and the same number of fog nodes. Each scene is covered by two cameras. Based on the index, we map the members of $\mathcal{S}$ and $\mathcal{S}'$ (i.e., the literals) to the cameras associated with the first $|\mathcal{S}|$ scenes. Thus, the i^{th} scene is monitored by the two cameras representing literals s_i and $\bar{s_i}$. The j^{th} clause in $\mathcal{D}$, i.e., d_j, is mapped to the two cameras with a view of the $(|\mathcal{S}|+j)^{th}$ scene. We denote these two cameras by d'_j and d''_j. The initial ages of the first $|\mathcal{S}|$ scenes and the remaining $|\mathcal{D}|$ scenes are a_0 and a_0+1, respectively. Each camera contains one image to be delivered. The maximum number of cameras supported by a fog node is uniformly set to two.

The transmit power of all cameras is uniformly set to one. For cameras s_i and $\bar{s_i}$, $i=1,2,\ldots,|\mathcal{S}|$, the SINR threshold is $\gamma_c=2$. For cameras d'_j and d''_j, $j=1,2,\ldots,|\mathcal{D}|$, the SINR threshold is $\gamma_c=\frac{1}{3}$. The noise power is $\sigma^2=0.5$ at the fog nodes 1 to $|\mathcal{S}|$, and $\sigma^2=1$ at the remaining $|\mathcal{D}|$ nodes. The channel gains between the cameras and the nodes are as follows.

$$G_{cn}=\begin{cases}1 & \text{if } c=s_i \text{ or } \bar{s_i},\ n=i,\ i=1,\ldots,|\mathcal{S}|;\\ 1 & \text{if } c=d'_j \text{ or } d''_j,\ n=|\mathcal{S}|+j,\ j=1,\ldots,|\mathcal{D}|;\\ \frac{1}{|\mathcal{S}|-1} & \text{if } c=s_i \text{ or } \bar{s_i},\ i=1,\ldots,|\mathcal{S}|,\ n=\\ & |\mathcal{S}|+1,\ldots,|\mathcal{S}|+|\mathcal{D}|, \text{ and } c \text{ is not one}\\ & \text{of the three literals of clause } d_{n-|\mathcal{S}|};\\ 0 & \text{otherwise.}\end{cases} \tag{8}$$

In what follows we show that the 3-SAT instance is satisfiable if and only if the above constructed MVAM instance has a feasible solution for the objective value a_0+2. By construction, we can observe that in a feasible solution the literal cameras s_i and $\bar{s_i}$ will be served by the fog node i, and the clause cameras d'_j and d''_j will be served by the fog node $|\mathcal{S}|+j$. Due to the SINR constraint, cameras s_i and $\bar{s_i}$ cannot transmit simultaneously, and consequently, at least two time slots are needed to deliver all images. Therefore, the minimum objective value for the MVAM instance is at least a_0+2. This is achieved if and only if a feasible solution with the following properties exists.

- All images are delivered in two time slots.
- Cameras s_i and $\bar{s_i}$ transmit in different time slots, and hence $|\mathcal{S}|$ literal cameras transmit simultaneously in each time slot.
- All the $2|\mathcal{D}|$ clause cameras transmit in the first time slot, together with $|\mathcal{S}|$ literal cameras. Due to the choice of the channel gains and transmit powers, for each clause, at least one camera representing one of its three literals transmit in the first time slot. Otherwise, suppose it is not the case for a clause, then the $|\mathcal{S}|$ literal cameras that transmit in the first time slot would all interfere with the two corresponding clause cameras. This, together with the interference they receive from each other, would result in an SINR $=\frac{1}{\frac{|\mathcal{S}|}{|\mathcal{S}|-1}+1+1}<\frac{1}{3}$.

Based on the above analysis, we established a mapping from the solution to that of the corresponding 3-SAT problem by setting all the literals represented by the cameras transmitting in the first time slot to be true, and the others to be false. Due to the third property, for the 3-SAT instance, every clause has at least one TRUE literal, and hence the 3-SAT instance is satisfiable. On the contrary, if the 3-SAT instance is satisfiable, then we map its solution to the corresponding MVAM problem by scheduling all the cameras representing the clauses and the TRUE literals in the first time slot, and the rest of the literal cameras in the second time slot. By doing so, we obtain a feasible solution of the MVAM instance with the objective value of a_0+2. Therefore, the 3-SAT instance is satisfiable if and only if there is a feasible solution for the corresponding MVAM with the objective value of a_0+2. Hence the decision problem of the MVAM is at least as hard as the 3-SAT problem. Since the 3-SAT problem is NP-complete, we conclude that the MVAM is NP-hard. ■

Observe that the MVAM under the physical model contains the subproblem of constructing feasible groups, which is akin to the so called *Link Activation (LA)* problem. Since LA itself is a hard problem [24], it is fundamental to understand whether the hardness of MVAM is merely a consequence of the hardness of LA. In the following theorem we provide a negative answer, stating that the MVAM is hard even if the candidate camera groups are given as problem input.

Theorem 2. *The MVAM with given candidate camera groups is NP-hard.*

Proof: We show the decision problem of the MVAM is NP-complete by constructing a polynomial reduction from the 3-SAT problem. We reuse the notation defined in the proof of Theorem 1. For an irreducible 3-SAT instance, we map the i^{th} positive literal s_i and its negation $\bar{s_i}$ to the two cameras monitoring the i^{th} scene, $i=1,2,\ldots,|\mathcal{S}|$. The j^{th} clause is mapped to the two cameras monitoring the $(|\mathcal{S}|+j)^{th}$ scene, $j=1,2,\ldots,|\mathcal{D}|$. Each camera contains one image to be delivered. The initial age of all scenes is uniformly set to a_0. The candidate camera groups consist of the following two subsets:

1) the $|\mathcal{S}|$ groups, of which the i^{th} group is formed by the two literal cameras s_i and $\bar{s_i}$, as well as the clause cameras that correspond to the clauses containing s_i as one of the three literals;
2) another $|\mathcal{S}|$ groups, of which the i^{th} group is formed by the two literal cameras s_i and $\bar{s_i}$, as well as the clause cameras that correspond to the clauses containing $\bar{s_i}$ as one of the three literals.

Since the 3-SAT instance is irreducible by assumption, the two subsets are disjoint. We remark that for any wireless network with meaningful physical interpretation, if a group is feasible then all of its proper subsets are feasible too. Hence the subsets of the above $2|\mathcal{S}|$ groups are also feasible. However, to achieve small peak ages, it is preferable to augment the subsets if possible and thus more images can be delivered in a time slot.

By construction, we observe that for any feasible solution of the MVAM instance, at least $|\mathcal{S}|$ time slots are consumed to deliver all the images, because images from different scenes in $\{1,2,\ldots,|\mathcal{S}|\}$ cannot be transmitted in a time slot. Consequently, the maximum peak age is at least $a_0+|\mathcal{S}|$, Suppose there is a solution achieving this objective value, then all the images are delivered in $|\mathcal{S}|$ time slots by groups belonging to either subset 1) or 2) defined above. We now establish

a solution mapping to the corresponding 3-SAT instance by setting a positive literal to be true if its corresponding camera transmits in a group of subset 1), and to be false if the corresponding camera transmits in a group of subset 2). It can be verified that by this solution, the 3-SAT instance is satisfiable since every clause contains at least one TRUE literal. One the contrary, if the 3-SAT instance is satisfiable, then the decision problem of the MVAM instance with the objective $a_0 + |\mathcal{S}|$ must be feasible. Hence we conclude that the MVAM with given candidate groups is at least as hard as the 3-SAT problem, and the theorem follows. ■

Finally, as a consequence of Theorem 2, we can also formulate the following result.

Corollary 3. *The MVAM under the protocol model is NP-hard.*

IV. Structural Results

In this section, we consider the MVAM for two baseline scenarios: a wireless camera network with interference-free channels and with severely interference-limited channels, respectively. In the first scenario, we consider that for each camera there exists at least one fog node such that the SINR exceeds its threshold when all cameras are active, thus the network allows all cameras to transmit simultaneously. This can be a reasonable model for emerging millimetre wave communications, and is also a good model for a system in which the cameras transmit with low power and each camera is deployed close to its serving fog node. The second scenario is the very opposite case in which only one camera is allowed to transmit in a time slot, i.e., it corresponds to time division multiple access (TDMA). This can be a reasonable model for severely interference-limited networks, e.g., when the cameras and nodes are densely deployed, and hence cameras cause significant interference to each other.

Not only do the two baseline scenarios represent two extremes of wireless channel condition, but they also result in classic channel access schemes that are easy to implement in practice. We are thus interested in investigating the tractability and optimality conditions of the MVAM problem for these two scenarios. We will show later that the structural results also contribute to the design of algorithms that efficiently compute or approximate an optimal solution for general MVAM cases.

Note that in our problem setup, the serving fog node of a camera is a decision variable. Therefore, for the two above baseline scenarios, all cameras transmitting simultaneously and TDMA might be infeasible for their corresponding MVAM instances, due to the requirement of multi-view processing and/or due to the fog node capacity constraint. In the following theorems we show that MVAM remains hard even for these two scenarios.

Theorem 4. *The MVAM problem in which all cameras transmit simultaneously is NP-hard.*

Proof: We establish a polynomial-time reduction from the partition problem, which is NP-complete [23]. Given a set of positive integers $\mathcal{I} = \{I_1, I_2, \ldots, I_S\}$, the partition problem is to determine whether or not $\mathcal{I}$ can be partitioned into two subsets with equal sum. Without loss of generality, we assume that $\sum_{I\in\mathcal{I}}$ is even, as otherwise it is trivial that the partition problem instance is infeasible. Let $\sum_{I\in\mathcal{I}} = 2b$ for some positive integer b. We construct an MVAM instance with S scenes $\mathcal{S} = \{1, 2, \ldots, S\}$ and two fog nodes $\mathcal{N} = \{n_1, n_2\}$. Each fog node supports at most b cameras. The s^{th} scene is monitored by I_s cameras. Each camera has one image to be delivered. The initial ages of the sources are uniformly set to a_0. Reusing the notation in Section II, we set the SINR threshold for camera c to $\gamma_c = \min\{\text{SINR}_{n_1}(c, \mathcal{C}), \text{SINR}_{n_2}(c, \mathcal{C})\}$, such that all cameras are possible to transmit concurrently. Then we consider the decision problem of the MVAM instance with the objective a_0+1. Define the binary variable $\iota_{sn} = \prod_{c\in\mathcal{c}(s)} l_{cn}$. That is, if the cameras $\mathcal{c}(s)$ are served by fog node n, then $\iota_{sn} = 1$. Otherwise, $\iota_{sn} = 0$. It is easy to verify that the objective $a_0 + 1$ is achieved if and only if there is an feasible fog-node assignment satisfying

$$\sum_{n\in\mathcal{N}} \iota_{sn} = 1 \quad \forall s \in \mathcal{S}, \tag{9a}$$

$$\sum_{s\in\mathcal{S}} |I_s|\iota_{sn} \leq b \quad \forall n \in \mathcal{N}. \tag{9b}$$

If such a solution exists, then (9b) are equalities since $\sum_{I\in\mathcal{I}} = 2b$. Thus we establish a solution mapping to the corresponding partition problem instance by partitioning $\mathcal{I}$ into two subsets $\mathcal{I}_1$ and $\mathcal{I}_2$ according to the value of ι_{sn}. Specifically, $\mathcal{I}_1 = \{I_s \in \mathcal{I} : \iota_{sn_1} = 1\}$, and $\mathcal{I}_2 = \{I_s \in \mathcal{I} : \iota_{sn_2} = 1\}$. Clearly, $\sum_{I\in\mathcal{I}_1} = \sum_{I\in\mathcal{I}_2} = b$. Therefore, the partition problem is feasible if the decision problem of the MVAM is feasible, and vice versa. Hence we conclude that the MVAM case defined in this theorem is at least as hard as the partition problem and the conclusion follows. ■

Theorem 5. *The MVAM problem in which only TDMA is allowed is NP-hard.*

The proof is omitted as it follows the same flow of arguments as the proof of Theorem 4, except that in constructing the corresponding MVAM instance, we set $\gamma_c = \min\{\text{SNR}(c, n_1), \text{SNR}(c, n_2)\}$, and the noise power σ_n is large enough such that only TDMA is allowed.

Remark 1. *In [6] we considered the age minimization problem where the number of cameras severed by a fog node is unlimited, and proved that the problem is computationally tractable if all cameras transmit simultaneously or if TDMA is applied. Theorems 4 and 5 show that the MVAM for the two baseline scenarios becomes NP-hard when imposing the constraints* (3)*. The theoretical results also provide the important insight that the optimization task of camera-node assignment is not trivial, even for given channel access schemes.* □

We now proceed to identifying tractable cases. For the above two baseline scenarios, we provide sufficient conditions for MVAM instances to be recognizable and solvable in polynomial-time.

Theorem 6. *Any MVAM instance in which each scene is monitored by the same number of cameras, i.e.,* $|\mathcal{c}(s)| = m$, $\forall s \in \mathcal{S}$, $m \in \mathrm{Z}^+$, *and all cameras are able to transmit*

simultaneously can be recognized and solved in polynomial-time.

Proof: To recognize the case defined in this theorem, given an MVAM instance, we construct a bipartite graph $\mathcal{G} = \{\mathcal{S}, \mathcal{N}, \mathcal{E}\}$, whose two disjoint vertex sets are formed by the scenes $\mathcal{S}$ and the fog nodes $\mathcal{N}$, respectively. We calculate the SINR value for each camera-node pair, with the assumption that all the cameras are transmitting, i.e., in the denominator of (4), the interference takes into account the signals from all other cameras. The computational complexity in this step is $O(CN)$. If for all cameras $c \in \boldsymbol{c}(s)$, the SINR between c and n exceeds its threshold then we add an edge connecting vertices s and n in graph $\mathcal{G}$. Obviously, if $M_n < m$, the problem instance is infeasible. If not, in graph $\mathcal{G}$, for each n, we add $\lfloor \frac{M_n}{m} \rfloor - 1$ dummy vertices, each of which is connected to the same vertices in $\mathcal{S}$ as n. Denote by $\mathcal{G}' = \{\mathcal{S}, \mathcal{N}', \mathcal{E}'\}$ the new bipartite graph after adding the dummy vertices and edges. By doing so, to determine whether or not there is feasible camera-node assignment such that all cameras are able to transmit simultaneously is equivalent to solving the *maximum matching problem* in the bipartite graph $\mathcal{G}'$. The matching problem reads

$$\max_{\{\iota_{sn} \in \{0,1\}\}} \quad \sum_{s \in \mathcal{S},\ n \in \mathcal{N}'} \iota_{sn} \tag{10a}$$

$$\text{subject to} \tag{10b}$$

$$\sum_{n \in \mathcal{N}} \iota_{sn} \leq 1 \quad \forall s \in \mathcal{S}, \tag{10c}$$

$$\sum_{s \in \mathcal{S}} \iota_{sn} \leq 1 \quad \forall n \in \mathcal{N}'. \tag{10d}$$

Bipartite matching can be solved in polynomial-time using, for example, the Hungarian algorithm [25]. If the objective of (10) equals $|\mathcal{S}|$, then we derive a feasible camera-node assignment such that all cameras can transmit simultaneously by setting $l_{cn} = \iota_{sn}$, $\forall c \in \boldsymbol{c}(s)$, and the MVAM instance is recognized.

The optimal transmission strategy for this case is straightforward, that is, in each time slot, all cameras transmit together as long as they have images in their queues. By (6), the optimal objective equals $t_0 + \max_{s \in \mathcal{S}, i \in \mathcal{K}_s}(i - \tau_{s,i-1})$, where $\mathcal{K}_s = \{1, \ldots, K_c\}$, $c \in \boldsymbol{c}(s)$. The computation can be done in polynomial-time and hence the conclusion. ■

For the MVAM with TDMA, i.e., no two cameras can transmit together, it is easy to see that the MVAM would be infeasible if TDMA is not allowed because of the multi-view processing requirement and the fog node capacity limit. Hence in deriving an optimal solution, we only consider feasible MVAM cases, where there exists an camera-node assignment that supports TDMA. Unlike for MVAM with all cameras transmitting simultaneously, determining the optimal transmission schedule of MVAM with TDMA is not trivial, we thus first establish a result concerning an optimal schedule.

Lemma 7. *Consider an instance of the MVAM with TDMA. There exits an optimal transmission schedule where the images in an image block, i.e., U_{ci}, $\forall c \in \boldsymbol{c}(s)$, are delivered in consecutive time slots.*

Proof: To prove the lemma, suppose Ω is an optimal solution in which images of an image block are not delivered in consecutive time slots. Denote by U_{ci}^{λ}, $\lambda = 1, \ldots, |\boldsymbol{c}(s)|$, the λ^{th} image of U_{ci}, $\forall c \in \boldsymbol{c}(s)$, delivered in Ω. We construct a new solution by moving all U_{ci}^{λ}, $\lambda = 1, \ldots, |\boldsymbol{c}(s)| - 1$, right before $U_{ci}^{|\boldsymbol{c}(s)|}$ and shifting the other images in between earlier in time. By doing so, the i^{th} peak age of s remains unchanged and the other peak ages (of s as well as the other sources) either remain unchanged or decrease. Hence the maximum peak age of the new solution is not higher than that of the previous solution. Repeating the operation for all image blocks that are not delivered in consecutive time slots we obtain a schedule Ω' that satisfies the lemma, and results in an age less than or equal to that of Ω, which proves the lemma. ■

We now use the optimal transmission schedule to show that the following MVAM case is tractable.

Theorem 8. *Any MVAM instance in which only TDMA is allowed and each scene is monitored by the same number of cameras, i.e., $|\boldsymbol{c}(s)| = m$, $\forall s \in \mathcal{S}$, $m \in \mathrm{Z}^+$, can be recognized and solved in polynomial-time.*

Proof: To recognize a TDMA instance, we first verify that no two cameras can transmit together. In the worst case, this can be done in $O(C^2N^2)$. To check whether there exists an feasible camera-node assignment to support TDMA, we follow an approach similar to the one in the proof of Theorem 6. Specifically, if $\frac{M_n}{m} < 1$, then the problem instance is infeasible. Otherwise, we construct a bipartite graph $G = \{\mathcal{S}, \mathcal{N}, \mathcal{E}\}$ in which two vertices (s, n) are connected if for all cameras $c \in \boldsymbol{c}(s)$, the SNR between c and n is above the threshold γ_c. If $\frac{M_n}{m} = 1$, then we solve the maximum matching problem in G and check if the result equals $|\mathcal{S}|$. If $\frac{M_n}{m} > 1$, then for each n, we add $\lfloor \frac{M_n}{m} \rfloor - 1$ dummy vertices that are connected to the same nodes in $\mathcal{S}$. An feasible assignment solution (if exists) is computed by solving the bipartite matching problem in the new graph, as defined in (10).

To construct an optimal transmission schedule, recall that by Lemma 7 there is an optimal solution in which the images in an image block are delivered consecutively. We now construct a schedule Ω, in which the image blocks B_{si}, $\forall s \in \mathcal{S}, i = 1, \ldots, K_c$, $c \in \boldsymbol{c}(s)$, are scheduled in ascending order of the time stamps $\tau_{s,i-1}$. The transmission order of the images in each image block is arbitrary. To show that Ω is optimal, we provide an indirect proof. Assume that Ω is not optimal. Then there is an optimal solution Ω_1, in which there exist two adjacent image blocks B_{si} and $B_{s'i'}$ with time stamps τ_{si} and $\tau_{s'i'}$, respectively, not transmitted in the defined order. That is, if $\tau_{s,i-1} > \tau_{s',i'-1}$, then B_{si} is transmitted before $B_{s'i'}$ in Ω_1. Denote by T_0 the time when the transmission of B_{si} starts, and by $|B_{si}|$ and $|B_{s'i'}|$ the number of images in B_{si} and $B_{s'i'}$, respectively. By (6b) and because of TDMA, the achieved peak ages by the two blocks are $\alpha_1 = T_0 + |B_{si}| - \tau_{s,i-1}$ and $\alpha_2 = T_0 + |B_{si}| + |B_{s'i'}| - \tau_{s',i'-1}$. Assume now that we swap the transmission of B_{si} and $B_{s'i'}$, obtaining a schedule Ω_2. Clearly, Ω_2 is feasible as it does not violate the FCFS discipline, and the peak ages of B_{si} and $B_{s'i'}$ change to $\alpha^3 = T_0 + |B_{s'i'}| - \tau_{s',i'-1}$ and $\alpha^4 = T_0 + |B_{s'i'}| + |B_{si}| - \tau_{s,i-1}$. Since $\tau_{s,i-1} > \tau_{s',i'-1}$, it can be easily verified that α^2 is maximal one among these four peak ages. Hence the maximal peak age in Ω_2 is either equal to

or less than that in Ω_1. Repeating the process for all adjacent image blocks that are not delivered in the defined order (cf. bubble sorting), after a finite number of steps, we obtain the transmission schedule Ω. According to the above analysis, the maximum peak age of Ω cannot be greater than that of Ω_1. This contradicts the assumption that Ω is not optimal, and hence the conclusion.

To construct the optimal transmission schedule, the bottleneck is to sort $\tau_{si}, \forall s \in \mathcal{S}, i = 0, 1, \ldots, K_c - 1, c \in \boldsymbol{c}(s)$. The computational complexity is hence $O(SK \log(SK))$, where $K = \max_{c \in \mathcal{C}} K_c$. As all the steps can be done in polynomial-time, the theorem follows. ∎

Note that by Theorem 8 and its proof, the optimal transmission strategy is determined solely by the values of the time stamps but not the number of images in each image block, i.e., $|B_{si}|$. Motivated by this observation, following a similar proof, we can extend the result of the optimal transmission schedule to a scenario in which only cameras monitoring the same scene can transmit simultaneously.

Corollary 9. *If no two cameras $c \in \boldsymbol{c}(s)$ and $c' \in \boldsymbol{c}(s')$, $s, s' \in \mathcal{S}$, $s \neq s'$, can transmit simultaneously, then in the optimal solution the images are delivered in ascending order of their last time stamps, and images of an image block are delivered in the same or consecutive time slots, depending on whether or not the corresponding cameras can transmit simultaneously.*

We can use this result for deriving a polynomial-time algorithm for MVAM instances where all cameras monitoring the same scene can transmit together.

Corollary 10. *Any instance of the MVAM in which only cameras $c \in \boldsymbol{c}(s)$, $\forall s \in \mathcal{S}$, are capable of transmitting together and each scene is monitored by the same number of cameras can be solved in polynomial-time.*

Proof: To assign the optimal fog node to each camera, we can follow a similar process as for the TDMA case. For each pair of $c \in \mathcal{C}$ and $n \in \mathcal{N}$, since $\boldsymbol{c}(s)$ are able to transmit together, we calculate the SINR value in which the interference is the sum of the signals from $\boldsymbol{c}(s) \setminus \{c\}$. Then the steps in the proof of Theorem 6 are used to derive the camera-node assignment. As for the case defined in the corollary, only $\boldsymbol{c}(s)$, $\forall s \in \mathcal{S}$, are feasible groups, i.e., no two cameras $c \in \boldsymbol{c}(s)$ and $c' \in \boldsymbol{c}(s')$, $s, s' \in \mathcal{S}$, $s \neq s'$, can transmit simultaneously, and thus by Corollary 9, the optimal transmission schedule follows directly. ∎

Finally, we provide a general optimality condition of the transmission schedule that applies to all MVAM instances.

Theorem 11. *Given a transmission schedule, let us denote by Λ_j the set of images delivered in time slot j, by T the schedule length, and let $\nu_j = min\{\tau_{s,i-1} : U_{ci} \in \Lambda_j, c \in \boldsymbol{c}(s)\}$. Then for any instance of the MVAM, there exists an optimal schedule in which ν_j, $j = 1, 2, \ldots, T$, are non-decreasing.*

Proof: See Appendix B. ∎

In Table II, we give a summary of the structural results.

TABLE II
SUMMARY OF STRUCTURAL RESULTS FOR THE MVAM PROBLEM.

MVAM case	Arbitrary number of cameras per scene	Same number of cameras per scene	Ref.
Under the physical model	NP-hard	NP-hard	Theorem 1
Under the protocol model	NP-hard	NP-hard	Corollary 3
With given candidate groups	NP-hard	NP-hard	Theorem 2
With all cameras transmitting together	NP-hard	tractable	For hardness: Theorem 4. For tractability: Theorem 6
With TDMA	NP-hard	tractable	For hardness: Theorem 5 For tractability: Lemma 7 and Theorem 8
Only cameras monitoring the same scene are capable of transmitting together	NP-hard	tractable	For hardness: Theorems 5. For tractability: Corollary 9 and Theorem 10

V. CORRELATED MAXIMUM AGE FIRST (CMAF) ALGORITHM

Inspired by the above structural results, in what follows we propose an efficient heuristic for the MVAM problem, called the *correlated maximum age first (CMAF)* algorithm. *CMAF* is based on a decomposition of the MVAM problem: it first solves the camera to node assignment problem, and for a given assignment it computes a transmission schedule.

A. Camera-node Assignment Algorithms

The *CMAF* uses two polynomial-time camera-node assignment algorithms. The first algorithm is based on the observation that in order to obtain the minimum peak age, in (6), T_{ci}, $\forall c \in \mathcal{C}$, $i = 1, \ldots, K_c$, should be as low as possible. This can be achieved if as many as possible cameras are active in each time slot. Therefore, the first algorithm aims at finding an assignment that maximizes the number of cameras that can transmit simultaneously.

It is worth noting that different from the classical maximum link activation problem [26], where only the SINR condition is considered, to support multi-view processing a feasible assignment solution must satisfy (2). In view of this, we start with constructing the weighted bipartite graph $\mathcal{G} = \{\mathcal{S}, \mathcal{N}, \mathcal{E}\}$. To create the edge set $\mathcal{E}$, we first check the "feasibility" of connecting each s and n in the graph $\mathcal{G}$. To do so, for each camera-node pair we calculate the SNR value. If for all $c \in \boldsymbol{c}(s)$ the SNR value exceeds its respective SINR threshold γ_c and node n is capable of supporting $\boldsymbol{c}(s)$, i.e., $M_n \geq |\boldsymbol{c}(s)|$, then we add an edge connecting s and n. Otherwise, the two vertices are disconnected, implying that either at least one camera that monitors s cannot transmit to n successfully even if it transmits alone or node n cannot serve all cameras for s. Next, in order to construct an assignment that maximizes the number of cameras that can transmit simultaneously, we define the weight $w_{sn} = \prod_{c \in \boldsymbol{c}(s)} \min\{1, \text{SINR}_n(c, \mathcal{C})/\gamma_c\}$ for each edge $(s, n) \in \mathcal{E}$. Intuitively, a higher value of w_{sn} implies that more cameras can be activated simultaneously. Based on the graph $\mathcal{G}$ we can formulate the following assignment problem.

$$\max_{\{\iota_{sn} \in \{0,1\}\}} \quad \sum_{s \in \mathcal{S},\ n \in \mathcal{N}} w_{sn} \iota_{sn} \tag{11a}$$

subject to (11b)

$$\sum_{n \in \mathcal{N}} \iota_{sn} = 1 \quad \forall s \in \mathcal{S}, \tag{11c}$$

$$\sum_{s \in \mathcal{S}} |\boldsymbol{c}(s)| \iota_{sn} \leq M_n \quad \forall n \in \mathcal{N}. \tag{11d}$$

The problem of (11) is the *Generalized Assignment Problem*, which is APX-hard [27], and even though a 2-approximation for GAP exists [28], it may not lead to a 2-approximation for the MVAM. We thus proceed with identifying two tractable cases. First, if $\sum_{s\in\mathcal{S}} |\mathcal{c}(s)| \leq M_n$, $\forall n \in \mathcal{N}$, then the conditions in (11d) are redundant. For this case, the optimal solution can be constructed by selecting the node $n = \text{argmax}_n\{w_{sn}, n \in \mathcal{N}\}$ as the serving node of cameras $c \in \mathcal{c}(s)$. Second, if $|\mathcal{c}(s)|$ is equal for all scenes, then (11) can be solved as a *maximum bipartite matching* following the approach stated in the proof of Theorem 6. To efficiently solve the general case, we apply the LR-Heuristic [29], which consists of the following steps.

1) For any $s \in \mathcal{S}$, if $|\mathcal{c}(s)| > M_n$, then we set the variable ι_{sn} to zero.
2) Solve the linear relaxation of (11).
3) Fix all variables that have value one and update (11). If any variable left, then go back to Step 1).

We refer to this algorithm as the *SINR-based assignment* algorithm.

The second algorithm is based on the observation that in the age calculation in (5), or equivalently, in (6b), small time stamps result in large peak ages. Thus, it is intuitively preferable to schedule "old" images as soon as possible, and the assignment should facilitate doing so. Consequently, we construct an assignment such that cameras containing images with small time stamps can transmit together. For a given MVAM instance, we first construct the weighted bipartite graph $\mathcal{G} = \{\mathcal{S}, \mathcal{N}, \mathcal{E}\}$, as before. For each $s \in \mathcal{S}$, we define the weight $w'_s = \frac{\tau}{\tau_{s1}}$, where $\tau = \min_{s\in\mathcal{S}}\tau_{s1}$. Thus, the weight is the scaled reciprocal of the minimum time stamp of all images taken for s. Finally, we update the weight of each edge $(s, n) \in \mathcal{E}$ to $w_{sn} = w'_s w_{sn}$. Given $\mathcal{G}$, we construct the assignment by solving the problem of (11), as in the case of *SINR-based assignment*. We refer to this as the *age-aware assignment* algorithm.

B. Transmission Scheduling Algorithm

Motivated by the structural results in Section IV, to deliver the images in a timely fashion, the cameras with images from an older source and carrying a smaller time stamp should be scheduled first. We thus propose a greedy strategy for the transmission schedule, which in each time slot chooses a camera group such that the image with the smallest time stamp and derived from the currently oldest scene is delivered together with as many other images as possible.

The algorithm works as follows. In each time slot, the camera group is initially empty. The algorithm first sorts the scenes $\mathcal{S}$ in the descending order of their current ages. Then the cameras monitoring each scene, i.e., $\mathcal{c}(s)$, are sorted in the ascending order of the time stamps of the images to be delivered, i.e., on the top of the queues. Ties, if any, are broken by the ascending order of scene/camera index. The algorithm adds the camera on the top of the list, that is, the camera associating with the most "aged" scene and carrying the image with the lowest time stamp, to the camera group. It then iterates through the ordered list of cameras, and adds one camera at a time. In each step, denote by $\mathcal{g}'$ the camera group with the new added camera c'. If $\text{SINR}_n(c, \mathcal{g}') \geq \gamma_c$, $\forall c \in \mathcal{g}'$, then the camera c' is kept; otherwise, c' is removed from the group. The algorithm schedules the computed camera group for transmission, after which it continues with the next time step, until all queues are empty.

C. Optimality of the CMAF Algorithm

The proposed *CMAF* algorithm uses the *SINR-based assignment* and *age-aware assignment* algorithms for computing two camera-node assignments. For both assignments, it executes the greedy scheduling algorithm described in Section V-B, and calculates the obtained maximum peak ages. The algorithm then chooses the camera-node assignment that results in lower maximum peak age. The pseudo-code of the *CMAF* algorithm is shown in Algorithm 1.

Algorithm 1 CMAF algorithm

Input: $\mathcal{S},\ \mathcal{C},\ \mathcal{N},\ \mathcal{M}_n,\ \mathcal{c}(s),\ \mathcal{K}_c,\ \tau_{si},\ a_{s0}$
Output: $\chi_1,\ \chi_2$

$feasible \leftarrow$ **true**, $\tau_{s0} \leftarrow t_0 - a_{s0},\ \forall s \in \mathcal{S},\ \chi \leftarrow \emptyset$
if $\sum_{n\in\mathcal{N}} M_n < \sum_{c\in\mathcal{C}} K_c$ **then**
  $feasible \leftarrow$ **false**, **return**
$\mathcal{G} \leftarrow \{\mathcal{S}, \mathcal{N}, \mathcal{E}\}, \mathcal{E} \leftarrow \emptyset$ // construct bipartite graph $\mathcal{G}$
for $c \in \mathcal{C}$ and $n \in \mathcal{N}$ **do** // SINR-based assignment
  calculate $\text{SNR}(c, n)$ and $\text{SINR}_n(c,\ \mathcal{C})$
for $s \in \mathcal{S}$ and $n \in \mathcal{N}$ **do**
  if $\text{SNR}(c, n) \geq \gamma_c, \forall c \in \mathcal{c}(s)$ and $M_n \geq |\mathcal{c}(s)|$ **then**
    $\mathcal{E} \leftarrow \mathcal{E} \cup \{(s, n)\}$, $w_{sn} \leftarrow \prod_{c\in\mathcal{c}(s)} \min\{1, \frac{\text{SINR}_n(c,\mathcal{C})}{\gamma_c}\}$
if $M_n \geq \sum_{s\in\mathcal{S}} |\mathcal{c}(s)|, \forall n \in \mathcal{N}$ **then**
  $\chi(c) \leftarrow \text{argmax}_n\{w_{sn}, n \in \mathcal{N}\}, \forall c \in \mathcal{c}(s)$
else if $M_n = m, \forall n \in \mathcal{N}$ **then**
  update G to G' by adding dummy nodes and edges; solve (10) using the Hungarian algorithm; update χ
else
  solve (11) using the LR-Heuristic; update χ
$\chi_1 \leftarrow \chi$
for $s \in \mathcal{S}$ and $n \in \mathcal{N}$ **do**
  $\chi \leftarrow \emptyset, \tau \leftarrow min_{s\in\mathcal{S}}\tau_{s1}, w'(s) \leftarrow \frac{\tau}{\tau_{s1}}, w_{sn} \leftarrow w'(s)w_{sn}$; repeat lines 10 to 15; $\chi_2 \leftarrow \chi$ // age-aware assignment

Input: $\mathcal{S},\ \mathcal{C},\ \mathcal{N},\ \mathcal{c}(s),\ \mathcal{K}_c,\ \tau_{si},\ a_{s0},\ t_0,\ \chi_1,\ \chi_2$
Output: $\chi*,\ \Omega*,\ \alpha^*$

$\chi \leftarrow \chi_1,\ \Omega_1 \leftarrow \emptyset,\ \alpha_1 \leftarrow 0$
$j \leftarrow 0,\ complete \leftarrow$ **false**, $empty(c) \leftarrow$ **false**, $\rho(c) \leftarrow 1,\ A(1) \leftarrow \{a_{s0}, s \in \mathcal{S}\}$ // maximum age first schedule
while $complete =$ **false do**
  $j \leftarrow j + 1,\ t \leftarrow t_0 + j,\ \mathcal{g}_j \leftarrow \emptyset$
  $\mathcal{C}' \leftarrow \mathcal{C}$ sorted first in descending order of $A(j)$ and then in ascending order of $\tau_{s,\rho(c)}$
  $\mathcal{g}_j = \{\mathcal{C}'(1)\}$
  for $r = 2, \ldots, |\mathcal{C}|$ **do**
    if $\text{SINR}_n(c,\ \mathcal{g}_j \cup \{\mathcal{C}'(r)\}) \geq \gamma_c$ **then**
      $\mathcal{g}_j \leftarrow \mathcal{g}_j \cup \{\mathcal{C}'(r)\}$
  $\Omega(j) \leftarrow \mathcal{g}_j,\ A(j + 1) \leftarrow \{a_{sj}, s \in \mathcal{S}\}$ computed by (5)
  for $c \in \mathcal{g}_j$ **do**
    if $\rho(c) < K_c$ **then**
      $\rho(c) \leftarrow \rho(c) + 1$
    else
      $empty(c) \leftarrow$ **true**
  if $empty(c) =$ **true** $\forall c \in \mathcal{C}$ **then**
    $complete \leftarrow$ **true**
$\alpha_1 \leftarrow max(A)$
$\chi \leftarrow chi_2,\ \Omega_2 \leftarrow \emptyset,\ \alpha_2 \leftarrow 0$; repeat lines 20 to 35; $\alpha_2 \leftarrow max(A)$
if $\alpha_1 \leq \alpha_2$ **then**
  $\alpha* \leftarrow \alpha_1,\ \Omega* \leftarrow \Omega_1,\ \chi* \leftarrow \chi_1$
else
  $\alpha* \leftarrow \alpha_2,\ \Omega* \leftarrow \Omega_2,\ \chi* \leftarrow \chi_2$
return $(\alpha*,\ \Omega*)$

Lemma 12. *The* CMAF *algorithm achieves the global optimum for the MVAM instances defined in Theorems 6 and 8, and in Corollary 10.*

Proof: For the three tractable cases, i.e., MVAM with compatible $\mathcal{C}$, MVAM with TDMA, and MVAM with compatible $\mathcal{C}(s)$ only, each stratifying $|\mathcal{C}(s)| = m$, $\forall s \in \mathcal{S}$, $m \in \mathrm{Z}^+$, by construction, both *SINR-based assignment* and *age-aware assignment* algorithms provide an optimal camera-node assignment. Together with the *transmission scheduling algorithm*, the *CMAF* gives the same result as the one we derived in the respective proof of the three theorems. ■

VI. Numerical Results

In this section we show simulation results to assess the potential benefit of adopting the fog architecture and of the proposed *CMAF* algorithm in terms of decreasing the maximum peak age of information.

A. Evaluation methodology

We consider a camera network monitoring an area of 100×100 meters, corresponding to an urban surveillance scenario. The area is divided into 16 sub-areas, each occupying 25×25 meters and consisting of one scene. The number of cameras that cover one scene is uniformly chosen on $[2, 6]$. For each scene s, the cameras $\mathcal{C}(s)$ are uniformly distributed in the respective sub-area. The transmit power of the cameras and the noise variance at the fog nodes are uniformly set to 20 dBm and to -100 dBm, respectively. The channel gain follows a distance-based propagation model with a path loss exponent of 4, Rayleigh fading, and log-normal shadowing with standard deviation of 6 dB [30]. The starting time is $t_0 = 500$. The initial ages a_{s0}, $\forall s \in \mathcal{S}$, are uniformly distributed in $[50, 200]$. Each camera has 10 images to be delivered. The time stamps of the images capturing scene s are integers uniformly distributed in $(t_0 - a_{s0}, t_0)$.

We generated 100 network instances with the above parameters for simulation. For each network instance, we deployed $N \in \{1, 2, 4, 8, 16\}$ fog nodes by splitting the area into N equal sized rectangles, and placing one fog node per rectangle. Depending on the location of the fog nodes with the rectangles, we distinguish between two topologies. In the regular topology, the fog node is located in the geometric center of the rectangle. In the random topology, the location of each fog node is chosen uniform at random in the respective rectangle. We set the maximum number of cameras that each fog node can support uniformly to $M_n = \frac{96}{N}$, $\forall n \in \mathcal{N}$. In Figure 5, we show the regular and the random topologies for $N = 16$ fog nodes in a network with $C = 59$ cameras.

As a baseline for comparison, we use the *location-based greedy (LBG)* algorithm. In *LBG*, the cameras are served by the nearest fog node, and for camera transmissions, a greedy algorithm for minimum time scheduling [31] is used. This greedy algorithm selects in each time slot the camera with maximal number of images left in queue and pairs it with other cameras that it can transmit together with. For performance comparison as well as for assessing the joint benefit of *CMAF* and fog computing in peak age reduction, we normalize all results by the maximum peak age achieved by *LBG* with $N = 1$, which corresponds to a traditional centralized network.

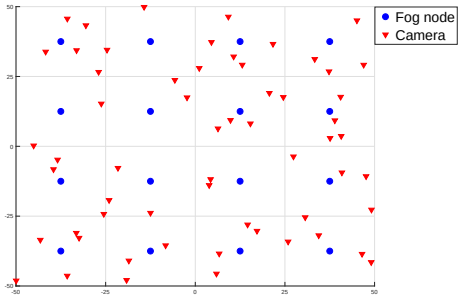

(a) Regular topology

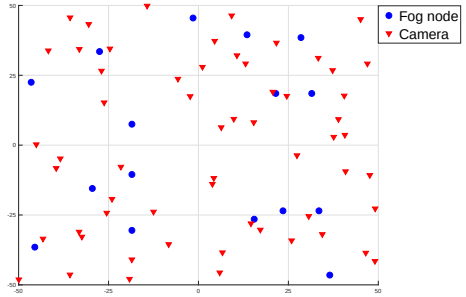

(b) Random topology

Fig. 5. A camera network with $N = 16$ fog nodes and $C = 59$ cameras.

B. Simulation Results

We first consider networks with low SINR thresholds. A low SINR threshold allows low bitrates, and since each camera in an active group transmits one image per time unit, this corresponds to camera networks where low image resolution is sufficient. In Figures 6a and 6c, we present the cumulative distribution function (CDF) of the normalized maximum peak age for networks with $\gamma = -3$ dB and $N \in \{1, 4, 16\}$, for the random and the regular topology, respectively. Each curve shows the results of 100 simulation runs.

Figures 6a and 6c show that *CMAF* outperforms *LBG* in terms of maximum peak age reduction for all values of N and for both topologies, by up to around 25%, depending on the network instance. Interestingly, for networks with a regular topology, shown in Figure 6c, the curves for *CMAF* for $N = 4$ and $N = 16$ almost overlap, indicating that a remarkable age reduction can be achieved by using only a small number of fog nodes if combined with *CMAF*, but the marginal gain of adding fog nodes decreases fast. Furthermore, the maximum peak age obtained using *CMAF* and $N = 4$ fog nodes is less than that obtained using *LBG* and $N = 16$ fog nodes.

Figures 6b and 6d show the average of the normalized maximum peak age as a function of the number of fog nodes for the two network topologies. The averages shown are computed based on the 100 network instances; we omitted the confidence intervals in the figures as they are within $\pm 2\%$ of the averages at 95% confidence level. The figures confirm the above observation, and show that adding fog nodes reduces the maximum peak age, but with a fast decreasing marginal gain. Comparing the results for *CMAF* and *LBG*, we can conclude that significantly less fog nodes are needed if using *CMAF* for achieving a given maximum peak age, allowing significant infrastructure savings compared to using *LBG*. Comparing the

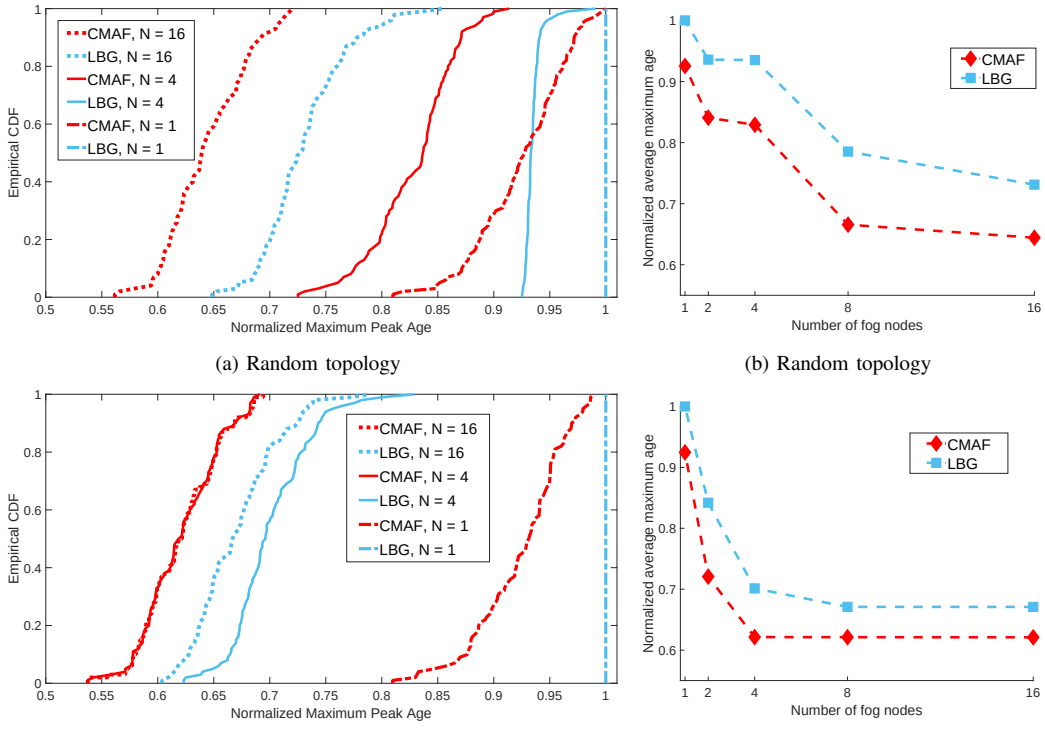

(a) Random topology (b) Random topology

(c) Regular topology (d) Regular topology

Fig. 6. Normalized maximum peak ages for networks with $\gamma = -3$ dB for random and regular topology.

results for the two topologies we can also observe that the age reduction is in general lower in case of the random topology. This is reasonable since the maximum peak age captures the worst case, which can be affected already by a few distant or co-located fog nodes, and suggests that if the number of fog nodes is relatively small then the placement of the fog nodes becomes very important.

Next, we consider systems with high SINR thresholds, i.e., camera networks that support services requiring high quality images. Figures 7a and 7c show the CDF of the normalized maximum peak age for the two network topologies with $\gamma = 13$ dB. In Figures 7b and 7d, we show the corresponding averages of the normalized maximum peak ages. The results are similar to the low SINR case in that *CMAF* achieves better performance in reducing the maximum peak age than *LBG*, in general, and allows significant savings in terms of the number of fog nodes to be deployed for guaranteeing a given maximum peak age. Comparing the results for different SINRs, we can observe that the gap between the results for $N = 4$ and $N = 16$ in the high SINR case (Figure 7) is larger than that in the low SINR case (Figure 6). The reason is that under high SINR requirements the fog nodes need to be closer to the cameras in order to allow simultaneous transmissions, and consequently a low age of information. Hence in comparison to the low SINR case, a dense fog node deployment would be more beneficial in high-speed camera networks. Overall, for both low and high SINR cases, the results show that the fog architecture combined with the proposed assignment and transmission strategy result in a synergy that significantly improves the freshness of information.

VII. Conclusions and Outlook

We have considered the joint optimization of serving node assignment and camera transmission scheduling with respect to age of information in wireless camera networks with fog computing. We have extended the age calculation in the presence of multi-view processing and mathematically formulated the multi-view age minimization problem. Fundamental results including problem complexity, tractable cases, and optimality condition have been derived. An optimization algorithm based on a modular structure has been proposed to solve the problem in polynomial time. Our numerical results show that the optimal assignment and transmission strategy reduces the maximum peak age significantly compared to the traditional centralized approach.

Our work has a number of interesting potential extensions, including optimizing the number and the placement of fog nodes, as well as determining the proper length of a scheduling cycle. It could also be interesting to consider images that arrive during a scheduling cycle for deriving an online optimal solution. If the cameras capture images periodically, or according to a known stochastic process, it may be feasible to jointly optimize the image update frequency and the transmission scheduling. As an example, in [14] the authors derived a separation principle to minimize the age of independent information for a Bernoulli arrival process. As an alternative, in lack of an arrival process model, one could develop a rolling horizon strategy where re-scheduling can take place during a cycle.

Our work also serves as a useful step towards designing a complete solution that minimizes age in an end-to-end sce-

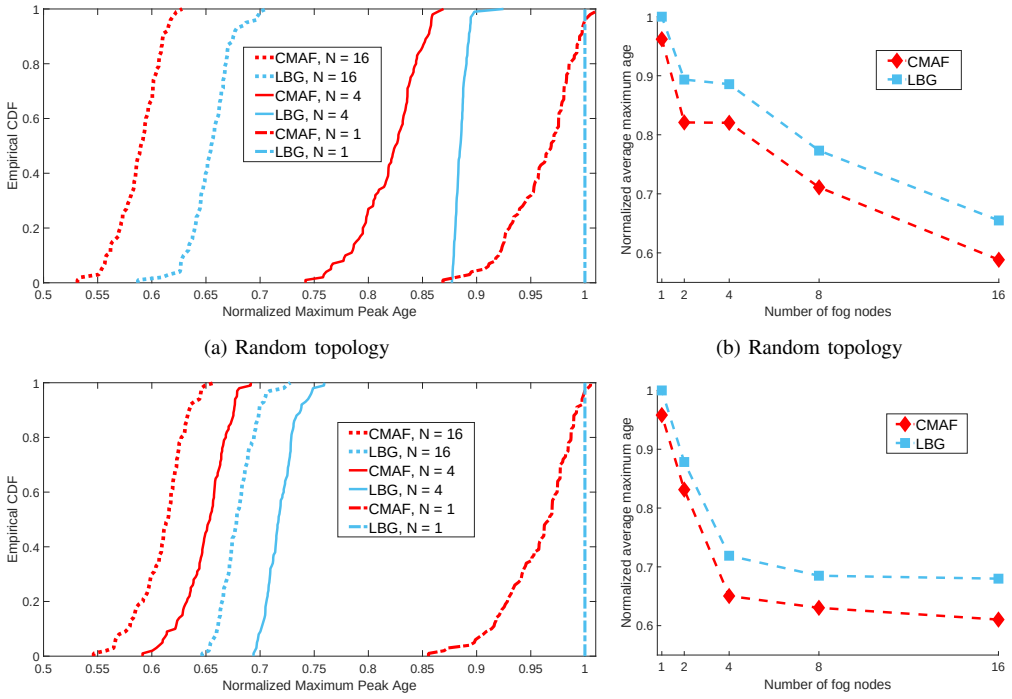

(a) Random topology (b) Random topology

(c) Regular topology (d) Regular topology

Fig. 7. Normalized maximum peak ages for networks with $\gamma = 13$ dB for random and regular topology.

nario, which involves the joint optimization of status update, queue management strategy, transmission scheduling, and data processing. These optimization tasks may take place at different locations, which makes the end-to-end optimization particularly challenging.

Appendix A
ILP for MVAM

We introduce the following binary variables.

$$x_{cij} = \begin{cases} 1 & \text{if image } U_{ci} \text{ is delivered at } t_j, \\ 0 & \text{otherwise.} \end{cases}$$

$$y_{sij} = \begin{cases} 1 & \text{if any image } U_{ci}, \forall c \in \boldsymbol{c}(s), \text{ is delivered at } t_j, \\ 0 & \text{otherwise.} \end{cases}$$

$$z_{sj} = \begin{cases} 1 & \text{if all images of cameras } \boldsymbol{c}(s) \text{ have been} \\ & \text{delivered before/at } t_j, \\ 0 & \text{otherwise.} \end{cases}$$

$$v_{sij} = \begin{cases} 1 & \text{if the last update of } U_{ci}, \forall c \in \boldsymbol{c}(s), \text{ is} \\ & \text{delivered at } t_j, \\ 0 & \text{otherwise.} \end{cases}$$

$$\iota_{sn} = \begin{cases} 1 & \text{if the cameras } c \in \boldsymbol{c}(s) \text{ are served by node } n, \\ 0 & \text{otherwise.} \end{cases}$$

Following the system model defined in Section II, one active camera delivers one image per time slot, hence the total time to deliver all queued images is at most $T = \sum_{c \in \mathcal{C}} K_c$. Letting $\mathcal{J} = \{1, 2, \ldots, T\}$, $K_c = \{1, 2, \ldots, K_c\}$, and $\mathcal{K}_s = \mathcal{K}_c$, $c \in \boldsymbol{c}(s)$, we formulate the MVAM as the ILP in (12).

Since peak ages are maximal points in the age evolution (see Figure 1), the objective is equivalent to minimizing the maximal achievable age for all sources during the schedule cycle, as defined in (12a) and (12b). The constraint sets (12c) and (12d) are linearizations of the age calculation stated in (5). By definition, if the last image of an image block B_{si} is not delivered at t_j, then $v_{sij} = 0$. For this source, if not all the images are emptied at the moment, i.e., $z_{sj} = 0$, then the corresponding constraint (12c) reads $a_{sj} \geq a_{s,j-1} + 1$. If either v_{sij} or z_{sj} (or both) equals one, the right-hand side of (12c) is negative because $a_{s0} + T$ is an upper bound of the age of s. In this case, the constraints in (12c) take no effect. If the last image of an image block B_{si} is delivered at t_j, v_{sij} takes the value one and (12d) is written as $a_{sj} \geq t_j - \tau_{si}$ when z_{sj} is zero. If $z_{sj} = 1$, i.e., all the images of s have been delivered, both (12c) and (12d) become satisfied. Note that there are no constraints on a_{sj} in (12e) - (12o) and the objective is to minimize the maximal value of a_{sj}. Therefore, at the optimum, for any constraint in (12c) and (12d) taking effect, equality holds. Hence, the constraint sets (12c) and (12d) together give the same result as defined in (5). The constraints in (12e) ensure the FCFS order of the queues, that is, the image $U_{c,i+1}$ can be transmitted only if U_{ci} has been delivered. In addition, by (12e), one camera delivers at most one image in each slot $j = 2, \ldots, T$. The transmission rate in the first time slot is governed by (12f). The inequalities in (12g) - (12j) achieve the effect that the auxiliary variables y_{sij}, z_{sj}, and v_{sij} indeed take the desired values. By (12g), y_{sij} takes value one if and only if at least one camera $c \in \boldsymbol{c}(s)$ delivers its i^{th} image at t_j. The value of v_{sij} is defined by (12h) and (12i). By definition, $v_{sij} = 1$ indicates that all the images of the i^{th} view of s have been delivered by t_j and there is U_{ci}, $\forall c \in \boldsymbol{c}(s)$, being delivered at t_j. Only when both conditions are fulfilled, the right-hand side of (12h), i.e., $\sum_{c \in \boldsymbol{c}(s)} \sum_{j'=1}^{j} x_{cij'} + y_{sij}$ achieves its maximal value $|\boldsymbol{c}(s)| + 1$. Otherwise, it is less

than this value, resulting that v_{sij} takes value zero. If the two conditions are satisfied, v_{sij} must be one to fulfil (12i). The values of z_{sj} are set by (12j), that is, $z_{sj}=1$ if and only if all images of source s are delivered by t_j. The constraints in (12k) state the fact that all the images are delivered eventually.

$$\underset{\{x_{cij},\ y_{sij},\ z_{sj},\ v_{sij},\ \iota_{sn},\ l_{cn}\in\{0,1\},\ a_{sj}\in Z^*\}}{\text{minimize}} \quad \alpha \tag{12a}$$

subject to

$$a_{sj}\leq \alpha \quad \forall s\in\mathcal{S},\ \forall j\in\{0\}\cup\mathcal{J}, \tag{12b}$$

$$a_{sj}\geq a_{s,j-1}+1-(\sum_{i\in K_s} v_{sij}+z_{sj})(a_{s0}+T) \quad \forall s\in\mathcal{S},\ \forall j\in\mathcal{J}, \tag{12c}$$

$$a_{sj}\geq t_j-\sum_{i\in\mathcal{K}_s}\tau_{si}v_{sij}-(1-\sum_{i\in\mathcal{K}_s} v_{sij}+z_{sj})t_j \quad \forall s\in\mathcal{S},\ \forall j\in\mathcal{J}, \tag{12d}$$

$$x_{c,i+1,j}\leq\sum_{j'=1}^{j-1} x_{cij'} \quad \forall c\in\mathcal{C},\ \forall i\in\mathcal{K}_c\setminus\{K_c\},\ \forall j\in\mathcal{J}\setminus\{1\}, \tag{12e}$$

$$\sum_{i\in\mathcal{K}_c} x_{ci1}\leq 1 \quad \forall c, \tag{12f}$$

$$\sum_{c\in\boldsymbol{c}(s)} x_{cij}\leq|\boldsymbol{c}(s)|y_{sij}\leq|\boldsymbol{c}(s)|\sum_{c\in\boldsymbol{c}(s)} x_{cij} \quad \forall s\in\mathcal{S},\ \forall i\in\mathcal{K}_c,\ \forall j\in\mathcal{J}, \tag{12g}$$

$$(|\boldsymbol{c}(s)|+1)v_{sij}\leq\sum_{c\in\boldsymbol{c}(s)}\sum_{j'=1}^{j} x_{cij'}+y_{sij} \quad \forall s\in\mathcal{S},\ \forall i\in\mathcal{K}_c,\ \forall j\in\mathcal{J}, \tag{12h}$$

$$(|\boldsymbol{c}(s)|+1)v_{sij}\geq\sum_{c\in\boldsymbol{c}(s)}\sum_{j'=1}^{j} x_{cij'}+y_{sij}-|\boldsymbol{c}(s)| \quad \forall s\in\mathcal{S},\ \forall i\in\mathcal{K}_c,\ \forall j\in\mathcal{J}, \tag{12i}$$

$$z_{sj}=\sum_{j'=1}^{j} v_{s,K_c,j'} \quad \forall s\in\mathcal{S},\ \forall j\in\mathcal{J},\ c\in\boldsymbol{c}(s), \tag{12j}$$

$$z_{sT}=1 \quad \forall s\in\mathcal{S}, \tag{12k}$$

$$\sum_{n\in\mathcal{N}}\iota_{sn}=1 \quad \forall s\in\mathcal{S}, \tag{12l}$$

$$l_{cn}=\iota_{sn} \quad \forall s\in\mathcal{S},\ \forall c\in\boldsymbol{c}(s),\ \forall n\in\mathcal{N}, \tag{12m}$$

$$\sum_{c\in\mathcal{C}} l_{cn}\leq M_n \quad \forall\ n\in\mathcal{N}, \tag{12n}$$

$$P_cG_{cn}+(2-l_{cn}-\sum_{i\in\mathcal{K}_c} x_{cij})Q_{cn}\geq \gamma_c(\sum_{c'\neq c}(P'_cG_{c'n}\sum_{i\in\mathcal{K}_{c'}} x_{c'ij})+\sigma_n^2) \quad \forall c\in\mathcal{C},\ \forall c\in\mathcal{N},\ \forall j\in\mathcal{J}. \tag{12o}$$

The optimization task of camera-node assignment is constrained by (12l) - (12n). The equalities in (12l) ensure that each camera set $\boldsymbol{c}(s)$ is served by a node. By the constraints in (12m) and the definition of l_{cn} in (1), all cameras in $\boldsymbol{c}(s)$ are connected to the same node. In (12n) we define the capacity limit for each fog node. The SINR constraints are defined by the inequalities in (12o), where Q_{cn} is a positive parameter that is large enough to guarantee that the corresponding constraint is satisfied if camera c does not transmit at this time slot, i.e., $\sum_{i\in\mathcal{K}_c} x_{cij}=0$, or n is not the intended node for c, i.e., $l_{cn}=0$. For this purpose, we set $Q_{cn}=\gamma_c(\sum_{c'\neq c}P'_cG_{c'n}+\sigma_n^2)$. When any constraint of (12o) becomes active, i.e., $\sum_{i\in\mathcal{K}_c} x_{cij}=l_{cn}=1$, the corresponding inequality reads $P_cG_{cn}\geq\gamma_c(\sum_{c'\neq c}(P'_cG_{c'n}\sum_{i\in\mathcal{K}_{c'}} x_{c'ij})+\sigma_n^2)$, of which the left-hand side is the signal strength of c and the right-hand side is the SINR threshold multiplied by the interference and noise at node n in the j^{th} time slot.

Appendix B
Proof of Theorem 11

Proof: Suppose Ω_1 is an optimal schedule where ν_j^1, $j=1,2,\ldots,T$, are not in the non-decreasing order. Then there exist at least two adjacent slots, say the j^{th} and $j+1^{th}$ slots, satisfying $\nu_j^1>\nu_{j+1}^1$. The FCFS queue policy implies that ν_j^1 and ν_{j+1}^1 are not time stamps of two images from the same camera, because otherwise Ω_1 is infeasible. Denote by $\mathcal{S}_j^1$ and $\mathcal{S}_{j+1}^1$ the sets of scenes whose images are delivered in the two time slots, respectively. By definition, at t_j the maximal age (not necessarily a peak age) of the scenes $\mathcal{S}_j^1$ is at least $t_j-\nu_j^1$. Likewise, the maximal age of $\mathcal{S}_{j+1}^1$ at t_{j+1} is at least $t_j+1-\nu_{j+1}^1$. Clearly, $t_j+1-\nu_{j+1}^1>t_j-\nu_j^1$ holds because $\nu_j^1>\nu_{j+1}^1$. Therefore, the maximum peak age of Ω_1 cannot be less than $t_j+1-\nu_{j+1}^1$. We swap the two groups $\mathcal{g}_j^1$ and $\mathcal{g}_{j+1}^1$ to get a new solution Ω_2. As the swapping takes place for two adjacent groups (instead of images), one can verify that Ω_2 is feasible and the same sets of images are delivered in the two time slots for both Ω_1 and Ω_2. Therefore, there is no impact on the peak ages of the scenes $\mathcal{S}\setminus\{\mathcal{S}_j^1\cup\mathcal{S}_{j+1}^1\}$, who have no image delivered in the two time slots. Moreover, since ν_j^1 and ν_{j+1}^1 are not time stamps of two images from the same camera, after the swapping, in Ω_2, we have $\nu_j^2\leq\nu_{j+1}^2$. We now consider the possible changes in age for scenes with an image delivered in one slot only, i.e., $\mathcal{S}_j^1\setminus\mathcal{S}_{j+1}^1$ and $\mathcal{S}_{j+1}^1\setminus\mathcal{S}_j^1$. For any $s\in\{\mathcal{S}_{j+1}^1\setminus\mathcal{S}_j^1\}$, clearly, its age won't be increased in Ω_2 since its images are delivered either at the same slot as in Ω_1 or earlier. For any $s\in\{\mathcal{S}_j^1\setminus\mathcal{S}_{j+1}^1\}$, the image $U_{ci}\in\{\Lambda_j^1: c\in\boldsymbol{c}(s)\}$, is scheduled one slot later after swapping. If U_{ci} is not the last delivered image of image block B_{si}, then there is no impact on peak age calculation. If it is the last delivered one in the image block, then in Ω_2, one peak age of s is achieved at t_{j+1}. By definition, the peak equals $t_{j+1}-\tau_{s,i-1}$. Obviously, in Ω_2, for the scenes $\mathcal{S}_j^1\setminus\mathcal{S}_{j+1}^1$, there is no peak age at t_j as they don't have any image delivered in the j^{th} time slot. Since the objective is the maximum age, we only need to compare the following (potential) peak ages in the two schedules. Recall that, in Ω_1, there is at least a maximal age $ma^1\geq t_{j+1}-\nu_{j+1}^1$. In Ω_2, the peak age at t_{j+1} is $ma^2=t_{j+1}-\tau_{s,i-1}$. By definition and the assumption, we have $U_{ci}\in\Lambda_j^1$ and $\nu_j^1>\nu_{j+1}^1$, hence $\tau_{s,i-1}\geq\nu_j^1>\nu_{j+1}^1$ holds, indicating $ma^1>ma^2$. Next, we consider the scenes $\mathcal{S}_j^1\cap\mathcal{S}_{j+1}^1$, which have images delivered in both slots. If $\mathcal{g}_j^1\cap\mathcal{g}_{j+1}^1=\emptyset$, then the above analysis for the scenes with image delivered only in one slot applies. If not, denote by U_{ci} and by $U_{c,i+1}$, $\forall c\in\{\mathcal{g}_j^1\cap\mathcal{g}_{j+1}^1\}$, the two

images delivered in the two slots, respectively. Depending on whether or not U_{ci} and/or $U_{c,i+1}$ are the last delivered image in their respective image block, as well as whether or not $\tau_{s,i-1} = \nu_j^1$ and/or $\tau_{s,i} = \nu_{j+1}^1$ hold, we check all possible combinations and calculate the potential changes in maximal age after the swapping. Following a similar approach as above, we conclude that in the new schedule Ω_2, the maximum peak age is either the same or less than that in Ω_1. Starting from Ω_1 and continuously swap any two adjacent groups that are not ordered as in the theorem, in each step, the objective is not getting worse and the new solution is feasible. The final solution we obtained follows the defined order and it is optimal. Hence the conclusion follows. ■

REFERENCES

[1] K. Abas, C. Porto, and K. Obraczka, "Wireless smart camera networks for the surveillance of public spaces," *IEEE Computer*, vol. 47, no. 25, pp. 37–44, 2014.

[2] B. S. et al., "Tracking and activity recognition through consensus in distributed camera networks," *IEEE Trans. Image Process.*, vol. 19, no. 10, pp. 2564–2579, 2010.

[3] J. K. et al., "Wireless sensor networks for healthcare," *Proc. IEEE*, vol. 98, no. 11, pp. 1947–1960, 2010.

[4] P. Papadimitratos, A. L. Fortelle, K. Evenssen, R. Brignolo, and S. Cosenza, "Vehicular communication systems: enabling technologies, applications, and future outlook on intelligent transportation," *IEEE Commun. Mag.*, vol. 47, no. 11, pp. 84–95, 2009.

[5] S. Kaul, R. Yates, and M. Gruteser, "Real-time status: How often should one update?" in *Proc. of IEEE INFOCOM*, 2012, pp. 2731–2735.

[6] A. Kosta, N. Pappas, and V. Angelakis, "Age of information: A new concept, metric, and tool," in *Foundations and Trends® in Networking*. Now Publishers, 2017.

[7] R. D. Yates and S. Kaul, "Real-time status updating: Multiple sources," in *Proc. of IEEE ISIT*, 2012, pp. 2666–2670.

[8] C. Kam, S. Kompella, and A. Ephremides, "Age of information under random updates," in *Proc. of IEEE ISIT*, 2013, pp. 66–70.

[9] S. K. Kaul, R. D. Yates, and M. Gruteser, "Status updates through queues," in *Proc. of IEEE CISS*, 2012, pp. 1–6.

[10] M. Costay, M. Codreanu, and A. Ephremides, "Age of information with packet management," in *Proc. of IEEE ISIT*, 2014, pp. 1583–1587.

[11] A. M. Bedewy, Y. Sun, and N. B. Shroff, "Age-optimal information updates in multihop networks," in *Proc. of IEEE ISIT*, 2017, pp. 576–580.

[12] Y. Sun, E. Uysal-Biyikoglu, R. D. Yates, C. E. Koksal, and N. B. Shroff, "Update or wait: How to keep your data fresh," *IEEE Trans. Inf. Theory*, vol. 63, no. 11, pp. 7492–7508, 2017.

[13] Q. He, D. Yuan, and A. Ephremides, "Optimal link scheduling that minimizes the age of information in wireless systems," *IEEE Trans. Inf. Theory*, vol. 64, no. 7, pp. 5381–5394, 2018.

[14] R. Talak, S. Karaman, and E. Modiano, "Optimizing information freshness in wireless networks under general interference constraints," in *Proc. of Mobihoc*, 2018.

[15] M. Chiang and T. Zhang, "Fog and IoT: An overview of research opportunities," *IEEE Internet Things J.*, vol. 3, no. 6, pp. 854–864, 2016.

[16] E. Eriksson, G. Dán, and V. Fodor, "Radio and computational resource management for fog computing enabled wireless camera networks," in *Proc. of IEEE GLOBECOM Workshop*, 2016, pp. 1–6.

[17] ——, "Predictive distributed visual analysis for video in wireless sensor networks," *IEEE Trans. Mobile Comput.*, vol. 15, no. 7, pp. 1743–1756, 2016.

[18] A. E. Redondi, L. Baroffio, M. Cesana, and M. Tagliasacchi, "Multi-view coding and routing of local features in visual sensor networks," in *Proc. of IEEE INFOCOM*, 2016.

[19] Q. He, G. Dán, and V. Fodor, "Minimizing age of correlated information for wireless camera networks," in *Proc. of IEEE INFOCOM Workshop*, 2018.

[20] P. Gupta and P. R. Kumar, "The capacity of wireless networks," *IEEE Trans. Inf. Theory*, vol. 46, no. 2, pp. 388–404, 2000.

[21] IBM, "IBM CPLEX Optimizer 12.6," http://www-01.ibm.com/software/commerce/optimization/cplex-optimizer/, 2015.

[22] GUROBI, "GUROBI Optimizer 6.5," http://www.gurobi.com/, 2015.

[23] M. R. Garey and D. S. Johnson, *Computers and Intractability: A Guide to the Theory of NP-Completeness*. W. H. Freeman, 1979.

[24] P. Värbrand and D. Yuan, "Resource allocation of spatial time division multiple access in multi-hop radio networks," in *Resource Management in Wireless Networking*, M. Cardei, I. Cardei, and D. Z. Zhu, Eds. Kluwer Academic Publishers, 2005, pp. 198–222.

[25] R. K. Ahuja, T. L. Magnanti, and J. B. Orlin, *Network Flows: Theory, Algorithms, and Applications*. Pearson Press, 2014.

[26] A. Capone, I. Filippini, S. Gualandi, and D. Yuan, "Resource optimization in multi-radio multi-channel wireless mesh networks," in *Mobile Ad Hoc Networking: Cutting Edge Directions*, 2nd ed., S. Basagni, M. Conti, S. Giordano, and I. Stojmenovic, Eds. Wiley and IEEE Press, 2013, pp. 241–274.

[27] C. Chekuri and S. Khanna, "A PTAS for the multiple knapsack problem," in *Proc. of ACM-SIAM SODA*, 2000, pp. 213–222.

[28] D. B. Shmoys and E. Tardos, "An approximation algorithm for the generalized assignment problem," *Math. Program.*, vol. 62, pp. 461–474, 1993.

[29] M. A. Trick, "A linear relaxation heuristic for the generalized assignment problem," *Naval Res. Logist.*, vol. 39, pp. 137–152, 1992.

[30] T. S. Rappaport, *Wireless Communications: Principles and Practice*. Prentice Hall, 2002.

[31] V. Angelakis, A. Ephremides, Q. He, and D. Yuan, "Minimum-time link scheduling for emptying backlogged traffic in wireless systems: solution characterization and algorithmic framework," *IEEE Trans. Inf. Theory*, vol. 60, no. 2, pp. 1083–1100, 2014.

Qing He (S'11–M'16) received the B.Sc. and M.Sc. degrees in electrical engineering from Nanjing University, China, in 2001 and 2004, respectively, and her Ph.D. degree from the Department of Science and Technology, Linköping University, Sweden, in 2016. She is currently a Post-Doctoral Researcher with the School of Electrical Engineering and Computer Science, KTH Royal Institute of Technology. She has a second degree in Finance and had been working as a software designer and system engineer in Lucent Technologies Bell Labs until 2011. Her current research interests include wireless network optimization, information theory, and machine learning.

György Dán (M'07-SM'17) is Professor at KTH Royal Institute of Technology, Stockholm, Sweden. He received the M.Sc. in computer engineering from the Budapest University of Technology and Economics, Hungary in 1999, the M.Sc. in business administration from the Corvinus University of Budapest, Hungary in 2003, and the Ph.D. in Telecommunications from KTH in 2006. He worked as a consultant in the field of access networks, streaming media and videoconferencing 1999-2001. He was a visiting researcher at the Swedish Institute of Computer Science in 2008, a Fulbright research scholar at University of Illinois at Urbana-Champaign in 2012-2013, and an invited professor at EPFL in 2014-2015. He has been an area editor of Computer Communications since 2014. His research interests include the design and analysis of content management and computing systems, game theoretical models of networked systems, and cyber-physical system security and resilience.

Viktoria Fodor (M'03–SM'13) is Professor of Communication Networks at KTH Royal Institute of Technology, Sweden. She received the M.Sc. and Ph.D. degrees from the Budapest University of Technology and Economics, Budapest, Hungary, in 1992 and 1999, respectively, both in computer engineering. She received habilitation qualification (docent) from KTH in 2011. In 1994 and 1995, she was a visiting researcher with Polytechnic University of Turin, Italy, and with Boston University, Boston, MA. In 1998, she was a senior researcher with the Hungarian Telecommunication Company. Since 1999, she has been with KTH. Viktoria Fodor's current research interests include performance evaluation of networks and distributed systems, stochastic modeling and protocol design. She has published more than hundred scientific publications, is associate editor of IEEE Transactions of Network and Service Management and Wiley Transactions on Emerging Telecommunications Technologies and area chair of IEEE Infocom 2019.